

Roughening Transition of a Restricted Solid-on-Solid Model in the Directed Percolation Universality Class

J. Ricardo G. de Mendonça*

Departamento de Física, Universidade Federal de São Carlos, 13565-905 São Carlos, SP, Brazil
(Physical Review E **60**, 1329–1336 (1999))

We carried out a finite-size scaling analysis of the restricted solid-on-solid version of a recently introduced growth model that exhibits a roughening transition accompanied by spontaneous symmetry breaking. The dynamic critical exponent of the model was calculated and found to be consistent with the universality class of the directed percolation process in a symmetry-broken phase with a crossover to Kardar-Parisi-Zhang behavior in a rough phase. The order parameter of the roughening transition together with the string order parameter was calculated, and we found that the flat, gapped phase is disordered with an antiferromagnetic spin-fluid structure of kinks, although strongly dominated by the completely flat configuration without kinks. A possible interesting extension of the model is mentioned.

PACS number(s): 64.60.Ht, 64.60.Ak, 05.70.Fh, 02.50.Ey

I. INTRODUCTION

It has been realized that nonequilibrium interacting particle systems are capable of exhibiting very interesting and unusual phenomena in (1+1) dimensions, such as single-defect and boundary induced phase transitions [1–3]. Moreover, it is known that some of these phase transitions are accompanied by spontaneous symmetry breaking (SSB) [3,4], in which some macroscopic observable of the model behaves in the steady state asymmetrically with respect to what it would be expected from the microscopic rules governing its dynamics. All this is rather unusual for equilibrium one-dimensional systems of particles interacting through short range forces only, and there have been serious attempts towards the understanding of these phenomena, in particular that of SSB [5]. It appears that among the many ingredients favoring SSB to take place, unbounded noise is a key one, whether it comes from the introduction of defects, boundary terms or any microscopic rules rendering a system lacking in detailed balance.

Growth models provide a suitable theoretical framework for the investigation of a gamut of model systems [6], and it turns out that they can be used to investigate the above mentioned phenomena as well. In a recent work [7], a class of growth models addressing both the questions of a roughening transition in one dimension and of SSB was introduced. Concerning SSB, these authors have inquired about the necessary ingredients in a model in order for it to show SSB, and they found it possible to have SSB characterized by a nonconserved order parameter in a ring geometry, as opposed to the situation in a related model showing the same characteristics but now with the SSB associated with a conserved (i.e., slow) order parameter and in the presence of conspicuous boundary terms [3,4]. In the unrestricted version, the models can be related to a directed percolation process thus sharing its exponents, a fact that was confirmed by Monte Carlo simulations [7]. In the restricted solid-on-solid (RSOS) version no such relationship exists. It is possible, however, to arrive through a site-link transformation at an equivalent driven diffusive system in which two types of oppositely charged particles diffuse asymmetrically and are continuously created and annihilated in pairs.

In this work we have proceeded to a further investigation of the RSOS version of the models first proposed in [7]. Our study is based on the mapping of the master equation governing the dynamics of the associated reaction-diffusion process into an imaginary-time Schrödinger equation, the Hamiltonian of which is that of a spin $S = 1$ non-Hermitian quantum chain [8]. This allows us to employ standard finite-size scaling (FSS) techniques to the resulting stochastic process, in the same way as one is used to do with Hamiltonian theories or with the transfer matrices of classical spins systems [9]. In this way we were able to analyze the time evolution operator for chains of sizes up to 16 sites, calculating their spectra and stationary states. The paper is organized as follows. In Sec. II we present the basic formalism in which we work, comment on its physical contents and derive the time evolution operator for the particular process we are interested in. In Sec. III we show and discuss the finite-size data we obtained for the dynamic critical exponent, the order parameter of the roughening transition, and the string order parameter. Finally, in Sec. IV we conclude and indicate some directions for further investigation.

II. THE TIME EVOLUTION OPERATOR

We are going to focus on the stochastic particle system associated with the growth model, more specifically on its stochastic transition or intensity matrix. There is quite a number of different ways of writing down the master equation in operator form, some more suited to the study of symmetries [8], some others envisaging a perturbative approach [10]. Here we give a brief derivation that parallels that of [8].

Let us attach to each site ℓ of a one-dimensional lattice $\Lambda \subset \mathbb{Z}$ of volume $|\Lambda| = L$ a stochastic variable n_ℓ taking values in the set of states $\omega = \{0, 1, \dots, N-1\}$. Denoting by $P(\mathbf{n}, t)$ the probability of realization of a particular configuration $\mathbf{n} = (n_1, n_2, \dots, n_L) \in \Omega = \omega^\Lambda$ at instant t , we write the master equation as

$$\frac{\partial P(\mathbf{n}, t)}{\partial t} = \sum_{\tilde{\mathbf{n}} \in \Omega} [\Gamma(\mathbf{n}, \tilde{\mathbf{n}})P(\tilde{\mathbf{n}}, t) - \Gamma(\tilde{\mathbf{n}}, \mathbf{n})P(\mathbf{n}, t)], \quad (1)$$

where $\Gamma(\tilde{\mathbf{n}}, \mathbf{n}) > 0$ is the rate for the transition $\mathbf{n} \rightarrow \tilde{\mathbf{n}}$. When only binary collisions intervene, we write $\Gamma(\tilde{\mathbf{n}}, \mathbf{n}) = \Gamma_{cd}^{ab}$ for the elementary process $(a, b) \rightarrow (c, d)$, and the master equation reads

$$\frac{\partial P(\mathbf{n}, t)}{\partial t} = \sum_{(\ell, m) \in \Lambda} \left[\sum_{a, b=0}^{N-1} \Gamma_{n_\ell, n_m}^{n_\ell+a, n_m+b} P(n_1, \dots, n_\ell + a, \dots, n_m + b, \dots, n_L, t) - \sum_{c, d=0}^{N-1} \Gamma_{n_\ell+c, n_m+d}^{n_\ell, n_m} P(\mathbf{n}, t) \right], \quad (2)$$

where the primes indicate that the free channel $(a, b) = (0, 0) = (c, d)$ should not be considered in the summations and the additions in the indices of the rates and in the arguments of $P(\mathbf{n}, t)$ are all taken modulo N . Periodic boundary conditions on Λ will be understood in what follows.

We now introduce vector spaces in the description of Eq. (2). To do this we turn $\omega = \{0, 1, \dots, N-1\}$ into $\omega = \mathbb{C}^N$ and \mathbf{n} into $|\mathbf{n}\rangle = |n_1, n_2, \dots, n_L\rangle \in \Omega = \omega^{\otimes \Lambda}$. Taking the orthonormal basis $\{|\mathbf{n}\rangle\}$ for Ω we write

$$|P(t)\rangle = \sum_{\mathbf{n} \in \Omega} P(\mathbf{n}, t) |\mathbf{n}\rangle \quad (3)$$

for the generating vector of the probabilities $P(\mathbf{n}, t) = \langle \mathbf{n} | P(t) \rangle$. We are in this way providing the space of generating functions with a Hilbert space structure. Next we endow the space of linear transformations of ω with the canonical basis of matrices E^{ab} with elements $(E^{ab})_{ij} = \delta_{ai} \delta_{bj}$, $0 \leq a, b, i, j \leq N-1$, and introduce the operator X such that $X_{ij} = \delta_{i+1, j}$, $X^N = \mathbf{1}$. A little reflection and comparison show that within this settings we can write Eq. (2) in the form

$$\frac{d|P(t)\rangle}{dt} = -H|P(t)\rangle \quad (4)$$

with

$$H = \sum_{(\ell, m) \in \Lambda} \sum_{a, b=0}^{N-1} \sum_{c, d=0}^{N-1} (1 - X_\ell^{a-c} X_m^{b-d}) \Gamma_{cd}^{ab} E_\ell^{aa} E_m^{bb}. \quad (5)$$

H is but the infinitesimal generator of the Markov semigroup $U(t) = \exp(-tH)$ of the continuous-time Markov chain defined by the set of rates Γ_{cd}^{ab} . From Eq. (5) we see that H is a $N^L \times N^L$, usually nonsymmetric, and very sparse matrix. One says that Eq. (4) is an imaginary-time Schrödinger equation, the fact that H has not the physical significance of energy and in general observes $H^\dagger \neq H$ notwithstanding. It is however useful and intuitive to think of H as a Hamiltonian whose quantum fluctuations govern the time fluctuations of the classical system of particles.

The process we are interested in is a growth model defined as follows [7]. Let $h_\ell \in \mathbb{N}$ be the height of a surface at site $\ell \in \Lambda$. The surface evolves by attempting, sequentially and at randomly chosen sites, adsorption of an adatom $h_\ell \rightarrow h_\ell + 1$ with probability qdt , and desorption of an adatom $h_\ell \rightarrow \min\{h_{\ell-1}, h_\ell\}$ or $h_\ell \rightarrow \min\{h_\ell, h_{\ell+1}\}$ each with probability $\frac{1}{2}(1-q)dt$. We now impose the RSOS condition $|h_{\ell+1} - h_\ell| \leq 1, \forall \ell \in \Lambda$, which suggests the use of link variables $c_\ell = h_{\ell+1} - h_\ell \in \{-1, 0, 1\}$. In order not to overload the notation with unnecessary pluses and minuses, let us take the values of c_ℓ modulo 3, mapping $c_\ell = -1, 0, 1$ into $c_\ell = 2, 0, 1$, respectively. In this representation the growth process can be described by the set of transition rates

$$\begin{aligned}
\Gamma_{01}^{10} &= \frac{1}{2}(1-q), & \Gamma_{10}^{01} &= q, \\
\Gamma_{02}^{20} &= q, & \Gamma_{20}^{02} &= \frac{1}{2}(1-q), \\
\Gamma_{00}^{12} &= 1-q, & \Gamma_{00}^{21} &= q, \\
&\text{and} & \Gamma_{12}^{00} &= q.
\end{aligned} \tag{6}$$

According to Eq. (5) we write for this process the time evolution operator as

$$H = \sum_{\ell=1}^L H_{\ell, \ell+1} \tag{7}$$

with the two-body stochastic transition matrix given explicitly by

$$H_{\ell, \ell+1} = \begin{pmatrix} q & \cdot & \cdot & \cdot & \cdot & -q & \cdot & -(1-q) & \cdot \\ \cdot & \frac{1}{2}(1-q) & \cdot & -q & \cdot & \cdot & \cdot & \cdot & \cdot \\ \cdot & \cdot & q & \cdot & \cdot & \cdot & -\frac{1}{2}(1-q) & \cdot & \cdot \\ \cdot & -\frac{1}{2}(1-q) & \cdot & q & \cdot & \cdot & \cdot & \cdot & \cdot \\ \cdot & \cdot & \cdot & \cdot & \cdot & \cdot & \cdot & \cdot & \cdot \\ \cdot & \cdot & \cdot & \cdot & \cdot & q & \cdot & \cdot & \cdot \\ \cdot & \cdot & -q & \cdot & \cdot & \cdot & \frac{1}{2}(1-q) & \cdot & \cdot \\ -q & \cdot & \cdot & \cdot & \cdot & \cdot & \cdot & 1-q & \cdot \\ \cdot & \cdot & \cdot & \cdot & \cdot & \cdot & \cdot & \cdot & \cdot \end{pmatrix}, \tag{8}$$

where we have ordered the two-site basis vectors antilexicographically, i.e., $|0,0\rangle \prec |1,0\rangle \prec \dots \prec |1,2\rangle \prec |2,2\rangle$, and the dots indicate null entries.

Before proceeding to the next section, it is worth mentioning some properties of H . As a stochastic transition matrix, conservation of probability flux requires $\sum_i H_{ij} = 0$, which in turn constraint the diagonal elements to be given by $H_{jj} = -\sum_{i \neq j} H_{ij}$, compare with Eq. (1). The first of these conditions imply the existence of a trivial left eigenstate with zero eigenvalue,

$$|\Omega\rangle = \sum_{\mathbf{n} \in \Omega} |\mathbf{n}\rangle, \quad \langle \Omega | H = 0, \tag{9}$$

with $\langle \Omega | \Omega \rangle = N^L$ the cardinality of the state space. This special vector plays a role in the determination of expectation values, for one can write the average of an observable $A(\mathbf{n})$ with respect to the probabilities $P(\mathbf{n}, t)$ with the aid of $|\Omega\rangle$ as

$$\langle A \rangle(t) = \sum_{\mathbf{n} \in \Omega} A(\mathbf{n}) P(\mathbf{n}, t) = \langle \Omega | A | P(t) \rangle. \tag{10}$$

We expect physical observables of the classical system of particles to be diagonal in the natural basis $\{|\mathbf{n}\rangle\}$, once they all have to commute. H is obviously not diagonal in this basis, it is not an observable of the system. Eq. (10) summarizes an important difference between quantum physics and the kind of classical physics we have here: it is that expectation values are linear in $|P(t)\rangle$, not bilinear, the elements of $|P(t)\rangle$ being probabilities themselves, not probability amplitudes.

Besides these general properties, our H in Eq. (7) is additionally translation invariant, due to the homogeneous rates in a ring geometry, and possesses a $U(1)$ symmetry labeled by the total charge $Q = Q^{(+)} - Q^{(-)}$, which is conserved along the process. These symmetries allow us to block-diagonalize H and to write it as the direct sum

$$H = \sum_{Q=-L}^L \sum_{k=0}^{L-1} H_k^Q, \tag{11}$$

where Q and k label the $U(1)$ and momentum eigensectors, respectively. Each $U(1)$ sector represents a closed class of the stochastic process, the corresponding block matrix H^Q being itself a stochastic transition matrix governing the dynamics within the given sector. We say that our process is decomposable, nonergodic, and that the $U(1)$ label classifies its $2L + 1$ irreducible, closed classes. The momentum label k , however, is introduced here solely in order

to take advantage, numerically, of the further reduction of order $1/L$ on the sizes of the blocks H^Q it furnishes, the physically relevant momentum sector being the one with $k = 0$, since the zero eigenvalue together with the completely flat surface of the model is in this sector. One can look for a relation $E(k) \propto k^\theta$ for the real part of the eigenspectrum, but we do not expect to extract useful information, e.g., about θ , from this relation for small lattice sizes. Moreover, the interpretation of such a relation for the low lying excitations of the process as a dispersion relation for quasiparticles of a free field theory would be somewhat cavalier; see [11,12].

III. FINITE-SIZE SCALING

According to Eqs. (6), as q increases creation of $+-$ as well as annihilation of $-+$ pairs increases while the remaining processes induce segregation of particles. This corresponds to an increase in adsorption and in the growth rate of islands, leading to rougher configurations. As q lowers, increased annihilation of $+-$ pairs together with more symmetric diffusion of 0's flatten the surface; see Sec. III C. Around the critical point $q = q_c$ separating these two phases the correlation lengths of the infinite system behave like

$$\xi_{\parallel} \propto \xi_{\perp}^{\theta} \propto |q - q_c|^{-\nu_{\parallel}} \propto |q - q_c|^{-\nu_{\perp}\theta}. \quad (12)$$

Here ξ_{\parallel} is the correlation length in the time direction while ξ_{\perp} is the one in the spatial direction, with ν_{\parallel} and ν_{\perp} the corresponding critical exponents and $\theta = \nu_{\parallel}/\nu_{\perp}$ the dynamic critical exponent.

For finite systems of size L , according to the usual FSS assumptions [9,13,14], we expect the scaling

$$\xi_{\parallel,L} \propto L^{\theta_L}, \quad (13)$$

to hold when $q = q_{c,L}$, the finite version of the critical point q_c , with θ_L the finite version of θ . On general grounds one expects $\lim_{L \rightarrow \infty} q_{c,L} = q_c$ and $\lim_{L \rightarrow \infty} \theta_L = \theta$. Therefore from Eqs. (12) and (13) we obtain the relations

$$\frac{\ln [\xi_{\parallel,L}(q_{c,L})/\xi_{\parallel,L-1}(q_{c,L})]}{\ln(L/L-1)} = \frac{\ln [\xi_{\parallel,L+1}(q_{c,L})/\xi_{\parallel,L}(q_{c,L})]}{\ln(L+1/L)} = \theta_L, \quad (14)$$

which through the comparison of three successive system sizes furnishes simultaneously $q_{c,L}$ and θ_L . Of course $\xi_{\parallel,L}^{-1} = \text{Re}\{\Delta E_L\}$, with $\Delta E_L = E_L^{(1)}$ the first gap of H , since for stochastic transition matrices $E_L^{(0)} = 0$ by construction.

A. Dynamic critical exponent

We have calculated the gaps ΔE_L in the $Q = 0$, $k = 0$ sector through the use of the Arnoldi algorithm [15,16]. This is a Krylov subspace projection technique that effects the reduction of a general nonsymmetric matrix to upper Hessenberg form, the eigenpairs of which converge variationally to that of the original matrix with the algebraically larger part of the spectrum converging first. In order to save memory we have used a restarted version of the algorithm, in which we fix the dimension of the Krylov subspace and use some of the approximate eigenvectors obtained in one iteration as the starting vectors for the next iteration, until convergence is obtained to the desired accuracy. In this way we were able to handle matrices of orders up to 324 862 with up to $\sim 8 \times 10^6$ nonzero entries keeping the Krylov subspace always with fewer than 64 vectors.

The results we have obtained are summarized in Tabs. I and II. The extrapolated values in the last line of these tables were obtained through the Bulirsch-Stoer extrapolation scheme [17], with ω_{BST} the free parameter of the algorithm chosen over a certain range so as to optimize the converge of the finite-size data.

In applying Eqs. (14) we found two consistent, converging sets of data, the first one, shown in Table I and marked with a prime, realizing the first equality in Eqs. (14) only approximately, and the second one, that in Table II and marked with two primes, realizing it exactly. This behavior is illustrated in Fig. 1.

The first set of data exhibited a rather smooth convergence in both the values of $q_{c,L}$ and θ_L , while the second set behaved more irregularly. The values in Table I indicate a second order transition taking place around $q'_c \simeq 0.1875$ with a dynamic exponent of $\theta' \simeq 1.585$. This value of θ' is compatible with the exponent of the directed percolation process, for which the most accurate value to date, obtained by Monte Carlo simulations, seems to be $\theta_{\text{DP}} = 1.58075(3)$ [18]; it should be mentioned that in an evaluation of θ_{DP} more closely related to ours it has been found a value of $\theta_{\text{DP}} = 1.588(1)$ [19], and that it is not clear why such discrepancies arise in the value of θ_{DP} calculated by different methods.

The interpretation of the data in Table II is touchier. We can see that the values of $q''_{c,L}$ converge at a reasonable rate to the extrapolated limit $q''_c \simeq 0.1932$, which is different from the previously found $q'_c \simeq 0.1875$. We believe however that if we had access to larger lattice sizes, we would have observed $q''_c \rightarrow q'_c$, since the values of q'_c vary less. We thus trust the value of $q'_c = 0.1875(1)$ as our best estimate for the critical point. The situation with the critical exponent θ''_L is different: it seems to be converging to a completely different value than θ_{DP} . In fact, this behavior was to be expected, for it has been found [7] that in the rough phase $q > q_c$ the exponents of the process are those of the Kardar-Parisi-Zhang universality class [20], in particular $\theta_{\text{KPZ}} = \frac{3}{2}$. As can be seen from Table II, the first few values of θ''_L show a monotonic increasing behavior up to $\theta''_9 \simeq 1.4649$, but then the sequence begins to decrease to reach the bottom value of $\theta''_{15} \simeq 1.4426$. A partial extrapolation of the first four points, $6 \leq L \leq 9$, gives $\theta'' = 1.47$, while a partial extrapolation of the rest of the points, $10 \leq L \leq 15$, gives $\theta'' = 1.42$. This absence of monotonicity of the finite-size data for θ''_L is quite unusual, and we have not yet a clear clue to this behavior. Even so, we can take the set of values of θ''_L in Table II as indicating the presence of a critical region for $q > q_c$ with an exponent $\theta'' \neq \theta_{\text{DP}}$, possibly with $\theta'' = \theta_{\text{KPZ}}$.

Concerning the exponent ν_{\perp} , we found it not possible to apply the standard approach [13,14] to obtain its value because the derivatives of $\text{Re}\{\Delta E_L\}$ with respect to q evaluated at the points $q_{c,L}$ change sign for some pairs of lattice sizes, thus preventing us from taking logarithms. The finite-size sequences obtained with the absolute values of these derivatives as well as with those obtained with the derivatives of the absolute values of the gaps also failed to converge, so that we were not able to obtain an estimate of ν_{\perp} from our diagonalizations.

B. Spontaneous symmetry breaking

Given that the surface suffers a transition from a flat phase to a rough phase, it is natural to think of an order parameter which measures this transition. Moreover, it is interesting to have an order parameter taking into account the symmetries of the process, which are besides the translational and $U(1)$ symmetries, a Z_{∞} symmetry related to the fact that the microscopic dynamics is invariant under an arbitrary integer shift $h_{\ell} \rightarrow h_{\ell} + n$ in the heights. A proper order parameter is given by [7]

$$M_L = \frac{1}{L} \sum_{\ell=1}^L (-1)^{h_{\ell}}, \quad (15)$$

which is fast in the sense of not being conserved by the dynamics. The choice of such an order parameter anticipates the interpretation of the roughening transition (actually, of the flattening transition) as the result of a spontaneous break of the Z_{∞} symmetry, for while in the rough phase all heights are exploited evenly, in the flat phase the system spontaneously selects one fiducial level around which the heights fluctuate. One then expects M_L to be finite in the flat phase while vanishing in the rough phase due to canceling fluctuations.

We have calculated M_L for even L between $L = 8$ and $L = 16$; our finite-size data together with the extrapolated values appear in Fig. 2. From that figure we clearly see the transition taking place around $q = 0.190$, although the precise determination of the critical point is not possible from this figure. We have not found the signature of two different q_c 's in our data for $M = \lim_{L \rightarrow \infty} M_L$, which we regard as an indication that q''_c should indeed tend to q'_c as $L \rightarrow \infty$.

The order parameter M vanishes around $q \lesssim q_c$ as $M \propto (q_c - q)^{\eta}$. The plot of $\ln M \times \ln(q_c - q)$ for the points $0.12 \leq q \leq 0.18$ of the extrapolated curve in Fig. 2 together with a linear regression fit appear in Fig. 3. We found an exponent $\eta = 0.57 \pm 0.03$, which compares well with previous results in the literature: in the first of the papers by Alon *et al.* [7], η has been evaluated as 0.55 ± 0.05 , while in a recent simulation of a model of yeastlike growth of fungi colonies with parallel dynamics it has been found that $\eta \simeq 0.50$ [21]. Also in a certain line in the phase diagram of a one-dimensional next-nearest-neighbor asymmetric exclusion process closely related to these growth models it has been found that $\eta = 0.54 \pm 0.04$ [22]. In the second of the papers by Alon *et al.* [7], however, the more accurate value $\eta = 0.66 \pm 0.06$ has been published, pushing the estimate to a somewhat higher value. Recent preliminary Monte Carlo simulations of ours, on the other hand, suggest a typical Ginzburg-Landau scenario for the symmetry break in these models, which would then predict an $\eta = \frac{1}{2}$. We believe that more extensive simulations can settle this point, and work is being done in this direction.

C. String order parameter

In order to better understand the nature of the roughening transition, let us look at some typical microscopic configurations of the model. The roughest possible surface is given in the links representation by $|++\cdots+--\cdots-\rangle$,

the state of maximal height in the $Q = 0$ sector of the dynamics. In spin language, this state corresponds to two domains separated by two antiferromagnetic (AF) kinks. The second roughest possible surface configurations are given by those with a pair of 0's, e.g., $|+\cdots+00-\cdots\rangle$ or $|0+\cdots+-\cdots-0\rangle$. From this example and the rates in Eqs. (6) it becomes clear that the flattening process is induced by AF kink annihilation, while diffusion of 0's introduce surface shape fluctuations. It is important to notice that absence of desorption from the middle of smooth terraces enforces a certain AF order among the particles, for pairs are created only as $+-$ pairs, never as $-+$ pairs, and since there are no $+- \rightleftharpoons -+$ reactions (which would violate the RSOS condition), we see that this order persists as long as pairs survive annihilation. In the rough, high q phase the $+$ particle will preferably move leftwards, while the $-$ particle will prefer to move to the right, eventually leaving a pair of 0's in between which then generates another $+-$ pair, thus leading to rough configurations like, e.g., $|\cdots++0\cdots-0-\cdots\rangle$. In the flat, low q phase diffusion of particles becomes more symmetric and segregation of particles less efficient, and we thus expect to observe a more uniform distribution of $+-$ pairs along the lattice than in the high q phase. The completely flat surface without any AF kink is only attained at $q = 0$.

In the context of two-dimensional RSOS crystal growth models and the Haldane conjecture [23], it has been predicted [24] and subsequently extensively verified [25–30] that a particular type of long-range order exists in the spin $S = 1$ antiferromagnetic isotropic Heisenberg (AFH) chain. In the ground state of the AFH chain, this order may be viewed as made up of (not necessarily closely) bound $+-$ dipoles interspersed among the 0's, forming what has become known as an AF spin fluid. The order parameter that identifies this type of order is the so-called string order parameter [24],

$$O_{\pi}^z(\ell) = \left\langle S_1^z \exp \left[i\pi \sum_{n=1}^{\ell} S_n^z \right] S_{\ell}^z \right\rangle, \quad (16)$$

where the brackets indicate expectation value in the ground state. In the gapped, Haldane phase of the AFH chain as well as in the disordered flat phase of the models in [24] one has $\lim_{\ell \rightarrow \infty} O_{\pi}^z(\ell) \neq 0$.

From what we said above it is clear that the string order is just the kind of order we expect to observe in the flat phase of our model. We have thus calculated the steady state expectation value of the string order parameter (16) with $S_n^z = c_n$ and $\ell = L/2 + 1$, the maximum distance in a ring geometry, and the results appear in Fig. 4. Our extrapolations did not perform well for this set of data, and are not showed in this figure. The general trend, however, is quite clear: above the critical point, $q > q_c$, $O_{\pi}^z(\ell)$ strongly tends to zero, while for $q \leq q_c$ we have $\lim_{\ell \rightarrow \infty} O_{\pi}^z(\ell) \neq 0$. The point $q = 0$ is special, for at $q = 0$ the completely flat surface becomes an absorbing state and $O_{\pi}^z(\ell) = 0$ exactly at this point. As q grows from zero, the AF spin fluid begins to form and $O_{\pi}^z(\ell)$ grows accordingly, until at $q = q_c$ the asymmetry in the diffusion rates for the particles disrupts this AF spin fluid structure, ordered domains begin to prevail and the string order vanishes. We then see that the string order parameter clearly reveals the mechanism of the roughening transition as the unbounding of the fluid antiferromagnetic pairs in favor of the formation of ordered domains.

IV. SUMMARY AND CONCLUSIONS

In summary, we carried out a finite-size scaling study of the roughening transition in a class of one-dimensional RSOS models which also presents spontaneous symmetry breaking. We found that at the critical point $q_c = 0.1875(1)$ the transition occurs with a dynamic exponent compatible with that of the directed site percolation process, for which we have the estimate $\theta = 1.585(1)$, and that above q_c there is a critical rough phase most probably with KPZ exponents. Unfortunately, we were unable to calculate a second exponent from our diagonalizations. This might be due to the nonhermiticity of the operator H , which might have caused an unusual nonmonotonicity in the values of the gaps with the parameter q , thus preventing us from obtaining ν_{\perp} . This lack of monotonicity has already been reported in the literature [4,31], where it has also been noticed the slow convergence of the finite-size data towards the infinite volume limit.

The order parameter M was found to vanish like $M \propto (q_c - q)^{\eta}$ for $q \lesssim q_c$ with an exponent $\eta = 0.57 \pm 0.03$, in agreement with previously found values of η [7,21,22]. The calculation of the string order parameter revealed that the flat, gapped phase of the model is a disordered phase analogous to a Haldane phase, with the stationary state presenting an antiferromagnetic spin-fluid structure of kinks, although dominated by the completely flat surface with no such a structure. The roughening transition may thus be understood in the links representation as the unbounding of the fluid antiferromagnetic pairs in favor of the formation of ordered domains, which then begin to blend together providing the surface with a finite growth velocity.

It is possible to push further the investigation of this class of models in one definite way. The idea is to allow for an explicit break of the symmetry in the set of rates Eq. (6) by the following artifact [32]. In the particle scenario,

we double the number of sites, introducing between two successive links $c_\ell, c_{\ell+1}$ a noninteracting flag variable $m_{\ell+\frac{1}{2}}$ taking two possible values, call them $+$ and $-$. This variable will mimic the pseudospin $(-1)^{h_\ell}$. We then allow the rates of our modified model to be parametrized by, besides q , a chiral symmetry breaking field $u \in [-1, 1]$ such that now the rates depend on the quantities

$$p = (1 - u)q \quad \text{and} \quad \tilde{p} = (1 + u)q$$

according to $\Gamma_{c-d}^{a+b} = \Gamma_{cd}^{ab}(p)$ and $\Gamma_{c+d}^{a-b} = \Gamma_{cd}^{ab}(\tilde{p})$, the roles of p and \tilde{p} interchanged whenever $\Gamma_{dc}^{ba} \neq 0$ for a given $\Gamma_{cd}^{ab} \neq 0$. For example, $\Gamma_{0-1}^{1+0} = \frac{1}{2}(1 - p)$ and $\Gamma_{0+1}^{1-0} = \frac{1}{2}(1 - \tilde{p})$, but $\Gamma_{1-0}^{0+1} = \tilde{p}$ and $\Gamma_{1+0}^{0-1} = p$. The choice of which combination of values of m 's in the new rates will pick a p or a \tilde{p} with respect to the original rates is immaterial, for letting $u \rightarrow -u$ exchange their roles. For this process one may look at the order parameter

$$M_L(u) = \frac{1}{L} \sum_{\ell=1}^L m_{\ell+\frac{1}{2}}$$

to see whether one finds a spontaneously symmetry-broken phase. It may happen that for some values of the field u one gets spinodal points, and that these points are associated with unusual dynamic exponents, e.g. $\theta = 1$, once they have already appeared in one dimensional driven diffusive systems [4]. This problem is currently under investigation.

ACKNOWLEDGMENTS

The author would like to acknowledge Professor Vladimir Rittenberg for having called his attention to this subject and Professor Francisco C. Alcaraz for helpful advice and many suggestions that greatly improved the final form of the manuscript. This work was supported by Fundação de Amparo à Pesquisa do Estado de São Paulo (FAPESP), Brazil.

-
- * Electronic address: jricardo@power.ufscar.br
- [1] J. Krug, Phys. Rev. Lett. **67**, 1882 (1991).
 - [2] D. Kandel and D. Mukamel, Europhys. Lett. **20**, 325 (1992); D. Kandel, G. Gershinsky, D. Mukamel, and B. Derrida, Phys. Scr. **T49**, 622 (1993).
 - [3] M.R. Evans, D.P. Foster, C. Godrèche, and D. Mukamel, Phys. Rev. Lett. **74**, 208 (1995); J. Stat. Phys. **80**, 69 (1995).
 - [4] P.F. Arndt, T. Heinzel, and V. Rittenberg, J. Stat. Phys. **90**, 783 (1998).
 - [5] C.H. Bennett and G. Grinstein, Phys. Rev. Lett. **55**, 657 (1985); P. Gács, J. Comput. Syst. Sci. **32**, 15 (1986); J.L. Lebowitz, C. Maes, and E.R. Speer, J. Stat. Phys. **59**, 117 (1990).
 - [6] T. Halpin-Healy and Y.-C. Zhang, Phys. Rep. **254**, 215 (1995); A.C. Levi and M. Kotrla, J. Phys.: Condens. Matt. **9**, 299 (1997).
 - [7] U. Alon, M.R. Evans, H. Hinrichsen, and D. Mukamel, Phys. Rev. Lett. **76**, 2746 (1996); Phys. Rev. E **57**, 4997 (1998).
 - [8] F.C. Alcaraz, M. Droz, M. Henkel, and V. Rittenberg, Ann. Phys. (N.Y.) **230**, 250 (1994).
 - [9] *Finite-size Scaling and Numerical Simulations of Statistical Systems*, edited by V. Privman (World Scientific, Singapore, 1990).
 - [10] L. Peliti, J. Phys. (Paris) **46**, 1469 (1985).
 - [11] M. Henkel and H.J. Herrmann, J. Phys. A **23**, 3719 (1990).
 - [12] J. Neergaard and M. den Nijs, Phys. Rev. Lett. **74**, 730 (1995).
 - [13] W. Kinzel and J.M. Yeomans, J. Phys. A **14**, L162 (1981); W. Kinzel, Z. Phys. B **58**, 229 (1985).
 - [14] B. Derrida and L. De Seze, J. Phys. (Paris) **43**, 475 (1982).
 - [15] W.E. Arnoldi, Quart. Appl. Math. **9**, 17 (1951); Y. Saad, SIAM (Soc. Ind. Appl. Math.) J. Sci. Stat. Comput. **5**, 203 (1984).
 - [16] G.H. Golub and C.F. Van Loan, *Matrix Computations*, 3rd ed. (The Johns Hopkins University Press, Baltimore, 1996).
 - [17] R. Bulirsch and J. Stoer, Numer. Math. **6**, 413 (1964); M. Henkel and G. Schütz, J. Phys. A **21**, 2617 (1988).
 - [18] I. Jensen, Phys. Rev. Lett. **77**, 4988 (1996); J. Phys. A **29**, 7013 (1996).
 - [19] D. ben-Avraham, R. Bidaux, and L.S. Schulman, Phys. Rev. A **43**, R7093 (1991).
 - [20] M. Kardar, G. Parisi, and Y.-C. Zhang, Phys. Rev. Lett. **56**, 889 (1986).
 - [21] J.M. López and H.J. Jensen, Phys. Rev. Lett. **81**, 1734 (1998).

- [22] D. Helbing, D. Mukamel, and G.M. Schütz, Phys. Rev. Lett. **82**, 10 (1999).
[23] F.D.M. Haldane, Phys. Lett. **93A**, 464 (1983); Phys. Rev. Lett. **50**, 1153 (1983).
[24] K. Rommelse and M. den Nijs, Phys. Rev. Lett. **59**, 2578 (1987); M. den Nijs and K. Rommelse, Phys. Rev. B **40**, 4709 (1989).
[25] S.M. Girvin and D.P. Arovas, Phys. Scr. **T27**, 156 (1989).
[26] H. Tasaki, Phys. Rev. Lett. **66**, 798 (1991).
[27] T. Kennedy and H. Tasaki, Phys. Rev. B **45**, 304 (1992); Commun. Math. Phys. **147**, 431 (1992).
[28] Y. Hatsugai and M. Kohmoto, Phys. Rev. B **44**, 11789 (1991); Y. Hatsugai, J. Phys. Soc. Jpn. **61**, 3856 (1992).
[29] F.C. Alcaraz and A. Moreo, Phys. Rev. B **46**, 2896 (1992); F.C. Alcaraz and Y. Hatsugai, Phys. Rev. B **46**, 13918 (1992).
[30] S.R. White and D.A. Huse, Phys. Rev. B **48**, 3844 (1993).
[31] E. Carlon, M. Henkel, and U. Schollwöck, Eur. Phys. J. B **00**, 0000 (1999).
[32] V. Rittenberg (private communication).

TABLE I. Finite-size data for the region where a minimum is observed. The numbers between parentheses represent the estimated errors in the last digit of the data.

$L - 1, L, L + 1$	$q'_{c,L}$	θ'_L
5,6,7	0.190 461(1)	1.794 411(1)
6,7,8	0.190 676(1)	1.749 008(1)
7,8,9	0.189 988(1)	1.718 350(1)
8,9,10	0.189 294(1)	1.695 320(1)
9,10,11	0.188 753(1)	1.677 170(1)
10,11,12	0.188 355(1)	1.662 589(1)
11,12,13	0.188 076(1)	1.650 766(1)
12,13,14	0.187 885(1)	1.641 112(1)
13,14,15	0.187 761(1)	1.633 190(2)
14,15,16	0.187 683(1)	1.626 655(2)
Extrapolated [ω_{BST}]	0.1875(1) [7.329]	1.585(1) [2.543]

TABLE II. Finite-size data for the region where crossing occurs. The data without an associated error are believed to be correct to the figures shown.

$L - 1, L, L + 1$	$q''_{c,L}$	θ''_L
5,6,7	0.295 749	1.445 967
6,7,8	0.275 660	1.458 235
7,8,9	0.261 781	1.463 535
8,9,10	0.251 648	1.464 937
9,10,11	0.244 053	1.463 830
10,11,12	0.238 186	1.461 059
11,12,13	0.233 511	1.457 203
12,13,14	0.229 689	1.452 672
13,14,15	0.226 497	1.447 753
14,15,16	0.223 784	1.442 647
Extrapolated [ω_{BST}]	0.1932(1) [1.815]	see text see text

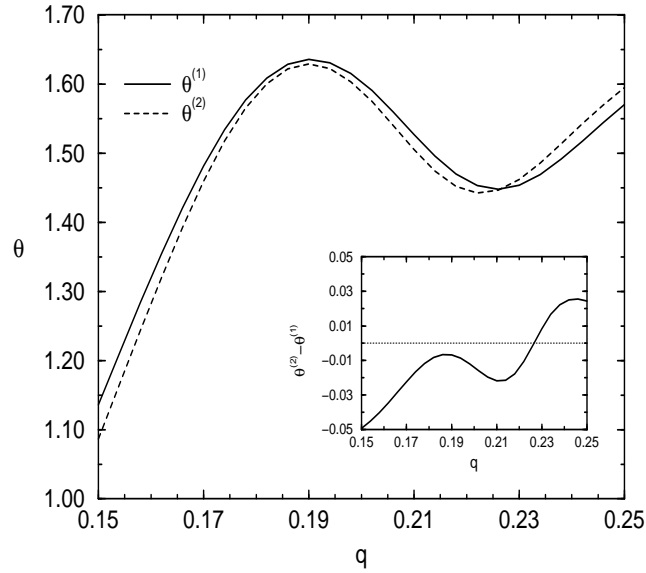


FIG. 1. Variation of the exponent θ with q . The values of $\theta^{(1)}$ and $\theta^{(2)}$ were obtained from the first and second expressions in Eqs. (14), respectively, using the triplet of lengths $L - 1, L, L + 1 = 13, 14, 15$. The inset shows that the difference between their values reaches a minimum around $q = 0.188$ and vanishes around $q = 0.226$. The finite-size sequences obtained from both the minima and the crossings converge to well defined limit values, see Tables I and II and the text.

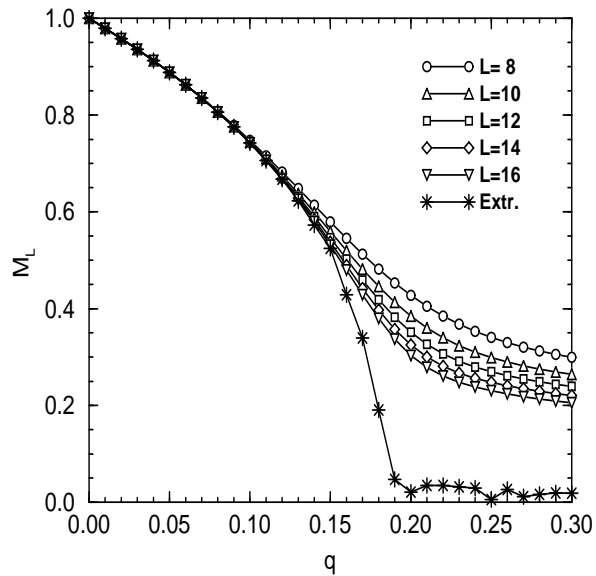


FIG. 2. Order parameter M_L for even L between $L = 8$ and $L = 16$ together with the extrapolated curve.

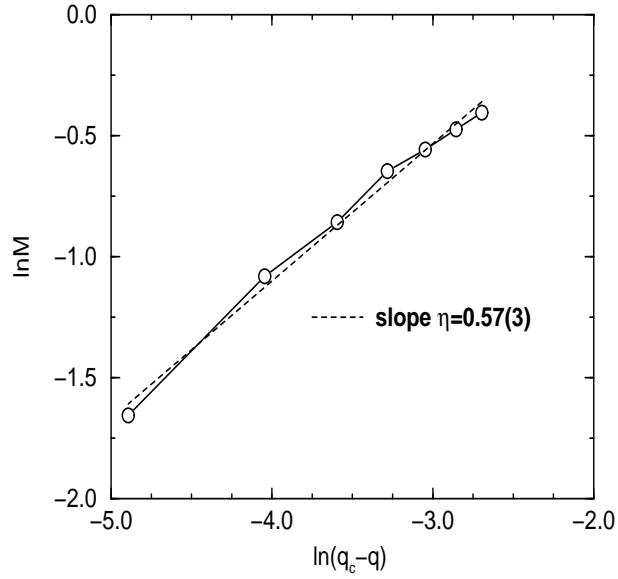


FIG. 3. Plot of $\ln M \times \ln(q_c - q)$. The LR slope gives the critical exponent $\eta = 0.57 \pm 0.03$.

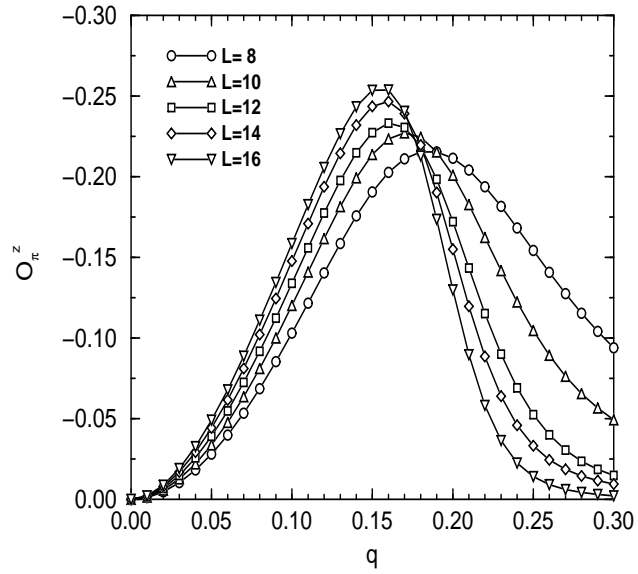


FIG. 4. String order parameter $O_\pi^z(L/2 + 1)$ for even L between $L = 8$ and $L = 16$.